Research, Society and Development, v. 10, n. 11, e77101119381, 2021
(CC BY 4.0) | ISSN 2525-3409 | DOI: http://dx.doi.org/10.33448/rsd-v10i11.19381

Three-dimensional study of the orbit-related structures according to sex, age and skeletal deformities

Estudo tridimensional das estruturas relacionadas à órbita de acordo com sexo, idade e deformidades esqueléticas

Estudio tridimensional de las estructuras relacionadas con la órbita según sexo, edad y deformidades esqueléticas

Received: 08/12/2021 | Reviewed: 08/17/2021 | Accept: 08/21/2021 | Published: 08/23/2021

Tamara Fernandes de Castro
ORCID: https://orcid.org/0000-0003-0870-8735
São Paulo State University, Brazil
E-mail: tamara_tfc@hotmail.com
Liogi Iwaki Filho
ORCID: https://orcid.org/0000-0001-9117-6826
State University of Maringá, Brazil
E-mail: liogifilho@gmail.com
Amanda Lury Yamashita
ORCID: https://orcid.org/0000-0001-8322-2060
State University of Maringá, Brazil
E-mail: amandayamashita@gmail.com
Fernanda Chiguti Yamashita
ORCID: https://orcid.org/0000-0002-1053-2559
State University of Maringá, Brazil
E-mail: nandayamashita@gmail.com
Naiara Caroline Aparecido dos Santos
ORCID: https://orcid.org/0000-0001-9117-6826
Federal University of São Carlos, Brazil
E-mail: naicaroline2@gmail.com
Eduardo Grossmann
ORCID: https://orcid.org/0000-0002-1238-1707
Federal University of Rio Grande do Sul, Brazil
E-mail: edugdor@gmail.com
Mariliani Chicarelli
ORCID: https://orcid.org/0000-0002-0024-7471
State University of Maringá, Brazil
E-mail: mchicarelli1@gmail.com
Lilian Cristina Vessoni Iwaki
ORCID: https://orcid.org/0000-0002-1822-3056
State University of Maringá, Brazil
E-mail: lilianiwaki@gmail.com

Abstract
Objective: This study aimed to evaluate the relations between orbit-related structures and sex, age and skeletal deformities using cone-beam computed tomography (CBCT). Methods: This retrospective study evaluated 216 consecutive CBCT scans of patients, who were divided according to: sex (male, n=105; female, n=111), age (A1: 18-32 years, n=71; A2: 33-47 years, n=78; A3: 48-62 years, n=67), and skeletal deformities (Class I, n=70; Class II, n=75; Class III, n=71). The supraorbital foramen (SOF) location, volume of orbit, optic canal (OC) and infraorbital canal (IOC) were evaluated. Results were analyzed using the Gamma model test. The Tukey-Kramer post-hoc test was used to compare the variables with three factors ($p<0.05$). Results: The IOC volume showed higher values for male, A3 and class I patients. The SOF location and the orbital volume also showed higher values for male patients. Regarding the volume of CO, it showed higher values for male and class I patients. Conclusions: According to our results, sex has been shown to have a significant influence on orbit-related structures. Age and skeletal deformities also influenced the volume of IOC and OC. These results eventually help the clinical practice, being useful for orbital reconstruction surgeries, anthropological studies, gender identification and identification of susceptibility to pathological conditions related to sexual dimorphism.
Keywords: Cone-beam computed tomography; Orbit; Sex characteristic.

Resumo

Objetivo: Este estudo teve como objetivo avaliar as relações entre estruturas orbitárias com o sexo, idade e deformidades esqueléticas por meio da tomografia computadorizada de feixe cônico (TCFC). Métodos: Este estudo retrospectivo avaliou 216 imagens consecutivas de TCFC de pacientes, que foram divididos de acordo com: sexo (masculino, n = 105; feminino, n = 111), idade (A1: 18-32 anos, n = 71; A2: 33 -47 anos, n = 78; A3: 48-62 anos, n = 67) e deformidades esqueléticas (Classe I, n = 70; Classe II, n = 75; Classe III, n = 71). Foram avaliados a localização do forame supraorbital (SOF), o volume da órbita, o canal óptico (CO) e o canal infraorbital (IOC). Os resultados foram analisados usando o teste do modelo Gamma. O teste post-hoc de Tukey-Kramer foi utilizado para comparar as variáveis com três fatores (p <0,05). Resultados: O volume do IOC apresentou valores maiores para os pacientes do sexo masculino, A3 e classe I. A localização do SOF e o volume orbital também apresentaram valores maiores para os pacientes do sexo masculino. Em relação ao volume de CO, este apresentou valores maiores para pacientes do sexo masculino e classe I. Conclusões: De acordo com nossos resultados, o sexo demonstrou ter uma influência significativa nas estruturas relacionadas à órbita. A idade e as deformidades esqueléticas também influenciaram o volume do COI e do CO. Esses resultados acabam auxiliando a prática clínica, sendo úteis para cirurgias de reconstrução orbitária, estudos antropológicos, identificação de gênero e identificação de suscetibilidade a condições patológicas relacionadas ao dimorfismo sexual.
Keywords: Tomografia computadorizada de feixe cônico; Órbita; Dimorfismo sexual.

Resumen

Objetivo: Este estudio tuvo como objetivo evaluar las relaciones entre las estructuras relacionadas con la órbita y el sexo, la edad y las deformidades esqueléticas mediante tomografía computarizada de haz cónico (CBCT). Métodos: Este estudio retrospectivo evaluó 216 exploraciones CBCT consecutivas de pacientes, que se dividieron según: sexo (hombre, n = 105; mujer, n = 111), edad (A1: 18-32 años, n = 71; A2: 33 -47 años, n = 78; A3: 48-62 años, n = 67) y deformidades esqueléticas (Clase I, n = 70; Clase II, n = 75; Clase III, n = 71). Se evaluó la ubicación del foramen supraorbitario (SOF), el volumen de la órbita, el canal óptico (OC) y el canal infraorbitario (IOC). Los resultados se analizaron mediante la prueba del modelo Gamma. Se utilizó la prueba post-hoc de Tukey-Kramer para comparar las variables con tres factores (p <0.05). Resultados: El volumen de IOC mostró valores más altos para los pacientes de sexo masculino, A3 y clase I. La ubicación de la SOF y el volumen orbitario también mostraron valores más altos para los pacientes masculinos. En cuanto al volumen de CO, mostró valores más altos para los pacientes del sexo masculino y clase I. Conclusiones: De acuerdo con nuestros resultados, se ha demostrado que el sexo tiene una influencia significativa en las estructuras relacionadas con la órbita. La edad y las deformidades esqueléticas también influyeron en el volumen de COI y CO. Estos resultados eventualmente ayudan a la práctica clínica, siendo útiles para cirugías de reconstrucción orbitaria, estudios antropológicos, identificación de género e identificación de susceptibilidad a condiciones patológicas relacionadas con el dimorfismo sexual.
Keywords: Tomografía computarizada de haz cónico; Orbita; Caracteres sexuales.

1. Introduction

The orbit is formed by the maxilla, frontal ethmoid, lacrimal, zygoma, sphenoid and palatine (Oppenheimer, Monson & Buchman, 2013). These are distributed along its walls. Its upper part consists of a part of the frontal bone and the lesser wing sphenoid; the inferior by the orbital plate of the maxilla, the orbital process of the zygoma and the orbital process of the palatine bone (Grob, Yonkers & Tao, 2017). Its medial wall is composed of the frontal process of the maxilla, orbital lamina of the ethmoid, orbital surface of the lacrimal bone, a part of the sphenoid bone. Its lateral wall encompasses the orbital process of zygoma and the orbital surface of the greater wing of the sphenoid (Norton, 2007; Hiatt & Gartner, 2001).

Orbital fractures are one of the most common injuries in midface trauma and can lead to significant functional and aesthetic complications (Manana, Odhiambo, Chindia & Koech, 2017). Orbital fractures may occur alone or in combination with other midfacial fractures, including fractures of zygomatic complex, naso-orbit-ethmoidal, frontal bone/orbital roof, Le Fort II and III (Dubois, Steenen, Gooris, Mourits & Becking, 2015). Isolated orbital fractures represent between 4% to 16% of facial skeletal injuries, while combined orbital fractures represent between 30% to 55% (Manana et al., 2017). Patients with fractures involving the orbit usually have concomitant injuries to the eyeball and/or the surrounding neurovascular structures, which include optic, infraorbital and supraorbital nerves (Sinanoglu, Orhan, Kursun, Inceoglu & Oztas, 2016). Thus, as the extent of orbital fractures increases, the risk of iatrogenic injury to neural and vascular structures also increases (Sinanoglu et al., 2016), making the treatment of orbital fractures challenging and complex (Andrades, Cuevas, Hernández, Danilla & Villalobos, 2018; Manolidis, Weeks, Kirby, Scarlett & Hollier, 2002).

Visual impairment, hypoesthesia of the infraorbital nerve, enophthalmia, irritating and persistent diplopia are considered complications of orbital fractures that are not managed properly (Manana et al., 2017). To avoid unwanted clinical results, orbital reconstruction surgery requires a complete assessment of orbital defects and the precise restoration of orbital dimensions and their surrounding structures (Yang & Liao, 2019). Therefore, a detailed preoperative radiograph evaluation and knowledge of these anatomical structures are necessary to obtain ideal results (Akdemir, Tekdemir & Altin, 2004).

For this reason, knowledge of the orbital volume and the relationship with clinical variables such as age and sex are important in the surgical decision-making process (Andrades et al., 2018). Furthermore, Friedrich et al. (2016) concluded that orbital volume measurements should be included in the follow-up control with special consideration of age- and gender-dependent changes in this parameter in orbital reconstructive surgeries. To the best of our knowledge, there are no studies that have evaluated the orbital volume and the structures that surround the orbit, such as the optic canal (OC), the infraorbital canal (IOC), the supraorbital foramen (SOF), and their relationship between sex, age and skeletal deformities. Thus, the aim of this study was to study the relations between orbit-related structures (orbital volume, OC volume, IOC volume, SOF location) and sex, age and skeletal deformities using cone-beam computed tomography (CBCT). The null hypothesis was that the orbit-related structures evaluated do not change according to sex, age and skeletal deformities.

2. Materials and Methods

This retrospective study was approved by the Ethics Committee for the Research Involving Human Beings of the State University of Maringá, Maringá, Brazil (CAAE 66291717.4.0000.0104). Due to the retrospective nature of this study, signed informed consent was not required. This study was also conducted according to the recommendations of the Strengthening the Reporting of Observational Studies in Epidemiology (STROBE) guidelines (von Elm, 2007).

Patients of both sexes, >18 years old and diagnosed with skeletal deformities (class I, II and III) were included in this study. Skeletal deformities were classified as class I (0º< ANB <4º), class II (ANB ≥ 4º), and class III (ANB < 0º) (Steiner, 1953). The exclusion criteria adopted in this study were: patients who underwent orthognathic surgery or any surgery on the middle third of the face, which could compromise the analysis of the structures of interest; patients who have craniofacial syndromes and congenital craniofacial anomalies.

The selected patients were divided according to: sex - male (M) and female (F); age - 18-32 years (A1), 33-47 years (A2) and 48-62 years (A3); and skeletal deformities - Class I (I); Class II (II); Class III (III).

Consecutive CBCT scans, which were requested for orthodontic or orthognathic surgery diagnosis and treatment planning, of 216 patients were obtained. All CBCT scans were carried out by the same specialist in oral and maxillofacial radiology and acquired with the i-CAT Next Generation® equipment (Imaging Sciences International, Hatfield, PA, USA). Volumes were reconstructed with an isometric voxel size of acquisition of 0.30 mm, FOV (Field of View) of 17 x 23 cm, tube tension of 120 kVp, and tube current of 3-8 mA. All CBCT scans were performed according to a strictly standardized scanning protocol; the patients were instructed to remain seated, adopt a natural head position, breathe lightly with their tongues and lips at rest, and stabilize their heads on a head and chin support.

The CBCTs were transferred into the Dolphin Imaging software version 11.95 (Dolphin Imaging & Management Solutions, Chatsworth, CA, USA) in DICOM (Digital Imaging and Communication in Medicine) format. The Dolphin software contains a tool for semi-automatic segmentation of the airways and its volume measurement, which is called sinus/airway. The sinus/airway tool was used to analyze the volume of the orbit, OC and IOC. This tool requires the user to define an area of interest by using some steps. First, the user must define, manually, the structure boundaries in the sagittal, axial and coronal reconstructions. Second, the user must place, manually, seed points in the destination compartment of the region of interest. The target volume will be filled automatically from those seed points; and all areas with similar grayscale intensity will also be selected, depending on the Hounsfield unit. Consequently, the threshold value must be determined. This limit defines a density range which will be included in the measured volume (de Water, Saridin, Bouw, Murawska & Koudstaal, 2014). The Hounsfield scale was adjusted and standardized, using the value of 400 HU for orbital volume (Nout et al., 2012), and the value of 70 HU for the OC and IOC volume.

In our study, the limits of each structure were standardized. For the orbital measurement, upper, lower, lateral, and medial limits are determined by the bone walls of the orbit. The anterior orbital margin was defined by a line between the most anterior point of the lateral bone limit and the most anterior point of the anterior lacrimal crest. The posterior limit is defined by the most anterior portion of the optical canal (Andrades et al., 2018; Friedrich, Bruhn & Lohse, 2016). For the OC measurement, the anterior and posterior bone limits of the canal were traced, taking into account the bone point defined more anteriorly and posteriorly in the minor wing of the sphenoid bone (Friedrich et al., 2016). For the IOC measurement, the anterior bone limits begin in the infraorbital foramen and the posterior margin of the IOC covered by the bone of the orbital floor (Fontolliet, Bornstein & Von Arx, 2019) (Figure 1).

Figure. 1. Delimitation and volume measurement (mm^3) of the orbit and surrounding structures. (A) Orbit. (B) Optic canal. (C) Infraorbital canal.

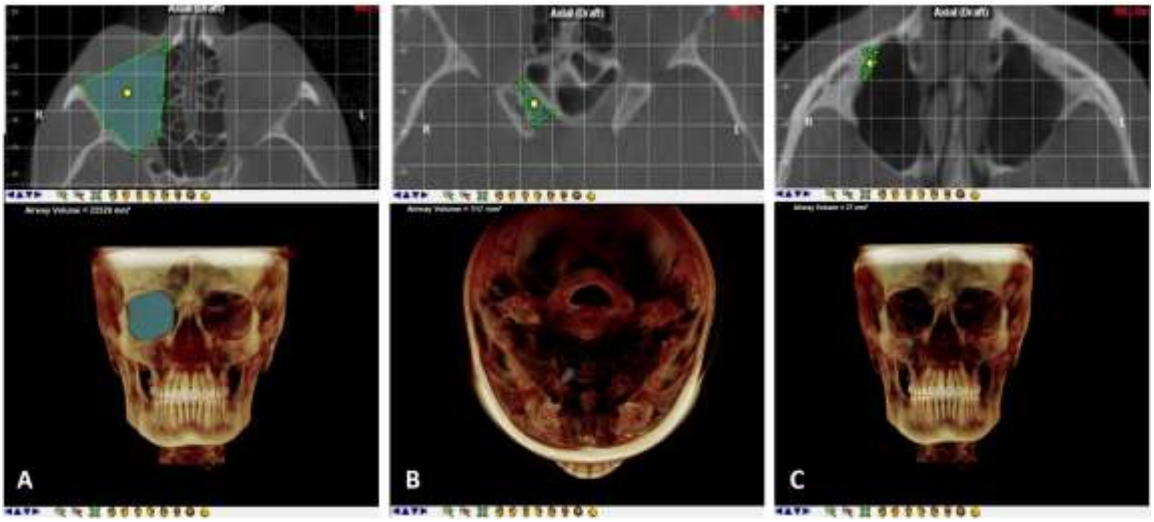

Source: Authors.

For the location of the SOF, the nasion point (N) was used as a reference. The distance from the center of the foramen to N was assessed on the right side (RN) and the left side (LN) (Sinanoglu et al., 2016) (Figure 2).

Figure 2. Illustration of the SOF location using nasion (N) as a reference. From N to SOF on the right side (RN) and left side (LN).

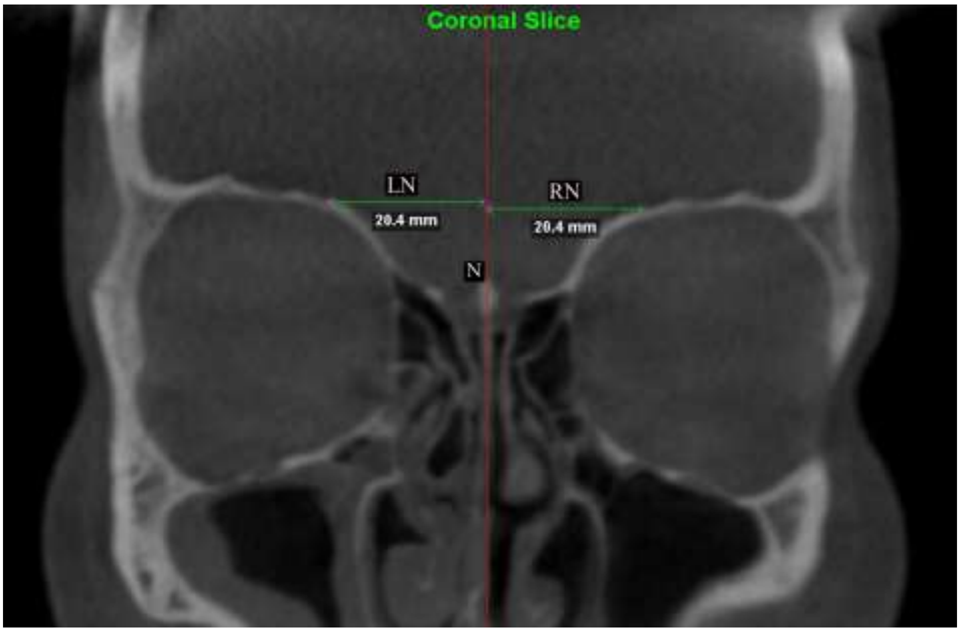

Source: Authors.

The images obtained were analyzed by one specialist in oral radiology, with experience in the analysis of tomographic images and the manipulation of image software. For the calibration process, 20% of CBCT scans were selected randomly and measurements were replicated twice with an interval of 15 days. Intra-examiner agreement was assessed by intraclass correlation coefficient (ICC). The generalized linear models (Gamma model) were used to evaluate the outcome variables (orbital volume, OC volume, IOC volume and SOF location) with sex, age and skeletal deformities. The Tukey-Kramer post-hoc test was used to compare the variables with three factors (age and skeletal deformities). All statistical tests were analyzed with R 3.1 software for Windows (R-project for statistical computing) at a 5% level of significance.

3. Results

The ICC value was good for all measurements, ranging from 0.732 to 0.941 (Koo & Li, 2016). The 216 scans were composed of 105 male and 111 female patients. Seventy-one individuals were between 18-32 years old; 78 were between 33-47 and 67 between 48-62. Regarding skeletal deformities, 70 individuals were classified as class I, 75 class II and 71 class III.

All the outcome variables (orbital volume, OC volume, IOC volume and SOF location) did not show statistically significant difference in terms of laterality ($p>0.05$). Therefore, these variables were not analyzed separately. The IOC volume displayed statistically significant difference between sex, age, and skeletal deformities. Male patients showed a larger volume when compared to female. The older group (A3) also exhibited a larger volume than the younger groups (A1 and A2) (Table 1). In addition, class I patients presented a statistically larger volume than class II and III (Table 2).

Significant statistical differences were noted between sex in SOF location and orbit volume, with higher values for male patients. Regarding the OC volume, significant statistical differences were observed between sex and skeletal deformities. Patients diagnosed with class I presented a larger volume than class II and class III (Table 2).

Table 1. Mean, standard deviation and p-values of SOF location and the volume of orbit, IOC and OC according to sex, age, and skeletal deformities.

	Male Mean±SD	Female Mean±SD	p-value	A1 Mean±SD	A2 Mean±SD	A3 Mean±SD	p-value A1-A2	p-value A1-A3	p-value A2-A3
Orbit volume	24586±2713	21685±1860	0.00*	23125±2702	23454±2810	23059±2445	0.33	0.63	0.32
IOC volume	32.5±12.4	26.6±5.6	0.00*	27.2±7.3	28.3±9.1	33.51±12.0	0.35	0.00*	0.00**
OC volume	113.5±19.7	105±14.1	0.00*	108.4±15.3	110.2±16.2	108.8±21.0	0.35	0.76	0.43
SOF distance	20.0±2.4	19.0±3.6	0.00*	19.3±3.7	19.3±2.8	19.8±2.6	0.79	0.17	0.22

*p-value based on Gamma model; **p-value based on Tukey-Kramer test. SD: standard deviation; M: male; F: female; A1: 18-32 years; A2: 33-47 years; A3: 48-62 years; IOC: infraorbital canal; SOF: supraorbital foramen; OC: optic canal. Source: Authors.

Table 2. Mean, standard deviation and p-values of SOF location and the volume of orbit, IOC and OC according to sex, age, and skeletal deformities.

	Class I Mean±SD	Class II Mean±SD	Class III Mean±SD	p-value I-II	p-value I-III	p-value II-III
Orbit volume	23451±2821	22890±2368	23351±2786	0.09	0.72	0.37
IOC volume	32.5±14	28.6±7.3	27.4±6.4	0.00*	0.00*	0.51
OC volume	116.8±20.9	106.4±12.7	104.4±15.7	0.00*	0.00*	0.38
SOF distance	19.2±2.6	19.4±3.3	19.8±3.3	0.35	0.05	0.55

*p-value based on Gamma model; **p-value based on Tukey-Kramer test. SD: standard deviation; Class I; II: Class II; III: Class III; IOC: infraorbital canal; SOF: supraorbital foramen; OC: optic canal. Source: Authors.

4. Discussion

All the outcome variables of our study showed statistically significant differences between sex. This can be ascribed to the fact that the analyzed structures present sexual dimorphism, which is in agreement with previous studies (Friedrich et al., 2016; Graillon, Boulze, Adalian, Loundou & Guyot, 2017; Erkoç, Öztoprak, Gümüş & Okur, 2015). According to Erkoç et al. (2015), the axial skeleton is larger in men than in women, which also affects the orbit and the surrounding structures. Thus, this can be useful for orbital reconstruction surgeries, anthropological studies and gender identification. Furthermore, susceptibility to pathological conditions has been found in women as a result of these size differences, such as the risk of optic nerve compression and myopia, especially in patients with skeletal deformities (Erkoç et al., 2015).

Identifying and preserving supraorbital and infraorbital foramina are important objectives in surgical and local anesthetic procedures (Aziz, Marchena, & Puran, 2000). In our study, we analyzed the IOC volume, which was higher in the older group (48-62 years) when compared to other age groups. Although no studies had analyzed the IOC volume per se, our results are in line with Fontolliet et al. (2019), which used linear measures to estimate the IOC. They reported that the length and height of the IOC were significantly greater in patients older than 61 years (Fontolliet et al., 2019). Accordingly, the increase in the IOC volume with age can be attributed to the posterior displacement of the maxilla and the lateral and inferior orbital border, which occurs in facial skeletal aging (Lambros, 2007; Lim, Min, Lee & Hong, 2016). In addition, patients in class I had higher IOC volume values than those in classes II and III, showing that in addition to age and sex influence the anatomy of the IOC, skeletal deformities should be considered.

Leaving vital structures such as the optic nerve intact is a challenge in the restoration of complex anatomical structures in craniofacial reconstructive surgery (Kim, Jung, Kim, Lee & Kim, 2013). In our study, we analyzed the volume of the OC in patients with different skeletal deformities, which makes our study unprecedented and may contribute to the characterization of this structure. Our results show that OC volume presents statistical differences according to skeletal deformities, being higher in class I patients than in class II and III patients.

The orbital volume in our study did not change significantly with age. Diverging from previous studies, which reported that the orbital volume increases with age in a continuous way (Ugradar & Lambros, 2019; Friedrich et al., 2016). The results of our study suggest that the bone of the orbit is dynamic throughout adult life and the clinical signs of periorbital aging maybe not due to orbital bone changes. The same explanation can be attributed to the OC volume in our study, suggesting that just as orbital bones are dynamic throughout adulthood.

In our study, the SOF location showed a non-significant increase in patients aged 48-62 years. Lim et al. (2016) observed that older patients displayed the supraorbital foramen significantly more distant from the midline, which indicates lateral translation of the frontal and maxillary bones with aging.

In our study, the measurement of the orbital volume was carried out due the fact that craniofacial reconstructive surgery has the fundamental principle of restoring facial symmetry, reconstructing the defective orbital wall, and restoring the appropriate orbital volume to mitigate restricted eye movements (Kim et al., 2013). However, differences in the orbital volume in relation to other studies have been noticed, which may be due, at least in part, to the different image sources used. Most studies were performed with computed tomography (Andrades et al., 2018; Diaconu et al., 2017). Currently, CBCT has been providing useful data for defining orbital pathologies, calculating orbital reconstructions, or anthropological studies (Friedrich et al., 2016). Moreover, the use of CBCT is considered adequate for the evaluation of the orbital volume, as long as reference points are defined to a closed surface for the calculations (Friedrich et al., 2016). For this reason, CBCTs were used in our study to assess the orbit and its adjacent structures, taking into account the standardization of bone limitations of all analyzed structures. This may also be responsible for the differences observed in the values of the orbital volume and other structures among the studies.

It is worth mentioning that our sample size is remarkable and very standardized, since all CBCT scans were cautiously conducted by a single radiologist with a standardized scanning protocol. However, the comparison between studies that evaluated orbit-related structures has been proven to be difficult, because there is no consensus in the literature with the methodologies. Previous studies used different delimitations of orbital borders and surrounding structures for measurement, which made it difficult to compare the volumetric data. Furthermore, the literature regarding the orbit and the surrounding structures is still scarce, especially with respect to skeletal deformities. The results of this study bring a new perspective for the anatomy of this region.

5. Conclusion

According to our results, sex has been shown to have a significant influence on orbit-related structures. Age and skeletal deformities also influenced the volume of IOC and OC. These results eventually help the clinical pratice, since this information could be useful for orbital reconstruction surgeries, anthropological studies, gender identification and identification of susceptibility to pathological conditions related to sexual dimorphism.

References

Akdemir, G., Tekdemir, I., & Altin, L. (2004). Transethmoidal approach to the optic canal: surgical and radiological microanatomy. *Surg Neurol*. 62(3): 268-274. 10.1016/j.surneu.2004.01.022.

Andrades, P., Cuevas, P., Hernández, R., Danilla, S., & Villalobos, R. (2018). Characterization of the orbital volume in normal population. *J Craniomaxillofac Surg*. 46(4): 594-599. 10.1016/j.jcms.2018.02.003.

Aziz, S. R., Marchena, J. M., & Puran, A. (2000). Anatomic characteristics of the infraorbital foramen: a cadaver study. *J Oral Maxillofac Surg*. 58 (9) : 992-996. 10.1053/joms.2000.8742.

de Water, V. R., Saridin, J. K., Bouw, F., & Murawska M. M., Koudstaal, M J. (2014). Measuring Upper Airway Volume: Accuracy and Reliability of Dolphin 3D Software Compared to Manual Segmentation in Craniosynostosis Patients. *J Oral Maxillofac Surg*. 72(1): 139-144. 10.1016/j.joms.2013.07.034.

Diaconu, S. C., Dreizin, D., Uluer, M., Mossop, C., Grant, M. P., & Nam, A. J. (2017). The validity and reliability of computed tomography orbital volume measurements. *J Craniomaxillofac Surg*. 45(9): 1552-1557. 10.1016/j.jcms.2017.06.024.

Dubois, L., Steenen, S. A., Gooris, P. J. J., Mourits, M. P., & Becking, A. G. (2015). Controversies in orbital reconstruction-I. Defect-driven orbital reconstruction: a systematic review. *Int J Oral Maxillofac Surg*. 44(3): 308-315. 10.1016/j.ijom.2014.12.002.

Erkoç, M. F., Öztoprak, B., Gümüş, C., & Okur, A. (2015). Exploration of orbital and orbital soft issue volume changes with gender and body parameters using magnetic resonance imaging. *Exp Ther Med.* 9(5): 1991-1997. 10.3892/etm.2015.2313.

Friedrich, R. E., Bruhn, M., & Lohse, C. (2016). Cone-beam computed tomography of the orbit and optic canal volumes. *J Craniomaxillofac Surg*. 44(9): 1342-1349. 10.1016/j.jcms.2016.06.003.

Fontolliet, M., Bornstein, M. M., & von Arx, T. (2019). Characteristics and dimensions of the infraorbital canal: a radiographic analysis using cone beam computed tomography (CBCT). *Surg Radiol Anat*. 41(2): 169-179. 10.1007/s00276-018-2108-z.

Graillon, N., Boulze, C., Adalian, P., Loundou, A., & Guyot, L. (2017). Use of 3D Orbital Reconstruction in the Assessment of Orbital Sexual Dimorphism and Its Pathological Consequences. *J Stomatol Oral Maxillofac Surg*. 118(1): 29-34. 10.1016/j.jormas.2016.10.002.

Grob, S., Yonkers, M., & Tao, J. (2017). Orbital fracture repair. *Semin Plast Surg.* 31(1): 31-39. 10.1055/s-0037-1598191.

Hiatt, J. L & Gartner, L. P. (2001) T*extbook of head and neck anatomy.* (3a ed.), Lippincott Willians & Wilkins.165-174p.

Kim, Y. H., Jung, D. W., Kim, T. G., Lee, J. H., & Kim, I. (2013) Correction of orbital wall fracture close to the optic canal using computer-assisted navigation surgery. *J Craniofac Surg.* 24(4): 1118-1122. 10.1097/SCS.0b013e318290266a.

Koo, T. K., & Li, M. Y. (2016). A guideline of selecting and reporting intraclass correlation coefficients for reliability research. *J Chiropr Med.* 15(2): 155-163. 10.1016/j.jcm.2016.02.012.

Lambros, V. (2007). Observations on periorbital and midface aging. Plast Reconstr Surg. 120(5): 1367-1376; discussion 1377. 10.1097/01.prs.0000279348.09156.c3.

Lim, J. S., Min, K. H., Lee, J H., et al. (2016). Anthropometric analysis of facial foramina in Korean population: a three-dimensional computed tomographic study. *Arch Craniofac Surg.* 17(1): 9-13. 10.7181/acfs.2016.17.1.9.

Manana, W., Odhiambo, W. A., Chindia, M. L., & Koech, K. (2017). The pattern of orbital fractures managed at two referral centers in Nairobi, Kenya. *J Craniofac Surg*. 28(4): 338-342. 10.1097/SCS.0000000000003579.

Manolidis, S., Weeks, B. H., Kirby, M., Scarlett, M., & Hollier, L. (2002). Classification and surgical management of orbital fractures: experience with 111 orbital reconstructions. *J Craniofac Surg.* 13(6): 726-737. 10.1097/00001665-200211000-00002.

Norton, N. S. (2007). *Atlas da cabeça e do pescoço.* Elsevier. 50-507p.

Nout, E., van Bezooijen, J. S., Koudstaal, M. J., Veenland, J. F., Hop, W. C. J., Wolvius, E. B., & van der Wal, K. G. H. (2012). Orbital change following Le Fort III advancement in syndromic craniosynostosis: quantitative evaluation of orbital volume, infra-orbital rim and globe position. *J Craniomaxillofac Surg.* 40(3): 223-228. 10.1016/j.jcms.2011.04.005.

Oppenheimer, A. J., Monson, L. A., & Buchman, S. R. (2013). *Pediatric orbital fractures. Craniomaxillofac Trauma Reconstr*. 6(1):9-20. 10.1055/s-0032-1332213.

Sinanoglu, A., Orhan, K., Kursun, S., Inceoglu, B., & Oztas, B. (2016). Evaluation of optic canal and surrounding structures using cone beam computed tomography considerations for maxillofacial surgery. *J Craniofac Surg*. 27(5): 1327-1330. 10.1097/SCS.0000000000002726.

Scolozzi, P., Jacquier, P., & Courvoisier, D. S. (2017). Can clinical findings predict orbital fractures and treatment decisions in patients with orbital trauma? Derivation of a simple clinical model. *J Craniofac Surg*. 28(7): 661-667. 10.1097/SCS.0000000000003823.

Steiner, C. C. (1953). Cephalometrics for you and me. *Am J Orthod*. 39(10): 729-755.

Ugradar, S., & Lambros, V. (2019). Orbital volume increases with age: a computed tomography-based volumetric study. *Ann Plast Surg*. 83(6): 693-696. 10.1097/SAP.0000000000001929.

von Elm, E., Altman, D. G., Egger, M., Pocock, S. J., Gøtzsche, P. C., Vandenbroucke, J. P., & STROBE Initiative. (2007). The Strengthening the Reporting of Observational Studies in Epidemiology (STROBE) statement: guidelines for reporting observational studies. *Bull World Health Organ.* 85(11): 867-872. 10.2471/blt.07.045120.

Yang, J. R., & Liao, H. T. (2019). Functional and aesthetic outcome of extensive orbital floor and medial wall fracture via navigation and endoscope-assisted reconstruction. *Ann Plast Surg.* 82(1S Suppl 1): S77-S85. 10.1097/SAP.0000000000001700.